Modelling and Simulation for Single Phase Low Voltage On-Board Charger for Plug-In Electric Vehicle (Pev) Charging Applications

Gaiffy Singla, Surya Prakash

Abstract: ***This paper mainly emphasis on modelling and simulation of charging of electric batteries through Single Phase On-board Bidirectional Charger for Electric Vehicles. The charger resides of: i) two AC-DC full bridge bidirectional boost converter (120V AC to 400V DC); and ii) a half bridge DC-DC buck converter. The AC to DC full bridge boost converter and DC-DC buck converter has been developed for charging purpose. The controller for both converters has been designed. The motive of AC-DC converter controller is to supervene the Active and Reactive Power (P-Q) commands provided by grid or utility. With the change in controllable commands the parameters of DC side can be adjusted. For each converter a separate controller is provided that maintains the balance between input power and output power. The controller for AC-DC converter helps to boost up the input grid voltage up to 400V DC. The charger must have to supervene the instructions/commands provided by grid or utility. The DC-DC converter is used to proselyte fixed voltage into variable voltage so that current required for charging the battery can be restrained. Work in this manuscript mainly focuses on Level-1 and Level-2 On Board charging system. The proposed single phase PEV charger is used to charge the Plug-in hybrid Electric Vehicles (PHEV) and Battery Electric Vehicles (BEV) in charging only operation. The charging system for EVs has been simulated and State of Charge (SOC) obtained are compared with the existing three developed charging systems.***

Index Terms: ***AC-DC Boost converter, Battery Charger, DC-DC buck converter, Plug-in Electric Vehicle, Unified Controller.***

I. INTRODUCTION

Electric Vehicles are growing very fast in today's environment and will remain in upcoming years. These are the best contrasting option to conventional Internal Combustion Engine (ICE) vehicles [1]. The electric vehicles are powered by an electric motor rather than petrol/diesel engine. So electric vehicles do not have any tailpipe and hence do not cause pollution. Large numbers of electric vehicles produce the congestion problem in distribution grid during peak load hours. So to overcome this problem, coordinated charging will be must to decrease the bad impact on grid [2], [3]. According to survey, the use of energy is going to elevate the transportation of world by 45% till 2030.The enhancement in the use of EVs is must to curb the climate change and to alleviate the oil fuel consumption. However, there are certain constraints regarding the acceptability of electric vehicles (EVs) because of capital cost, operating costs and deficient infrastructure for charging systems. The research work on PEVs is still on the way to bring major advancement in near future.

However, the EV charger shown in here comprises two converters that share a DC link. The charger is power linkage device that links the grid to vehicle. The DC link is used to connect these two converters. DC link plays a vital role in charging of battery from grid-to-vehicle. AC to DC transformation of power is carried out with the help of charger. The only purpose of charger is to follow Power commands that are provided by grid or utility/user. These commands are of various types which will be explained further. In recent days the reactive power that is consumed at utility grid is compensated via synchronous condensers, capacitor banks, etc. The transmission of reactive power from source to load causes a lot of transmission and distribution losses and reactive power at supply end is not equal to reactive power at load end. The transmission and distribution losses put pressure on distribution transformer that leads to decrease the voltage profile at distribution transformer side. To reduce the losses, it is favourable to generate the reactive power near to the load. For this purpose, On-Board chargers are the most preferable for providing high efficiency. The PEV charger can likewise satisfy the power quality functions; for example, compensation of reactive power, regulation of voltage, filtering of harmonics and power factor correction [4].

The prime motive of the charger is that it has to charge the electric vehicle battery through proper coordination between EV and grid. V2G (Vehicle to Grid) operation can also takes place by using bidirectional PEV charger. There is a need of giving reactive power back to grid amid peak load times. During peak load times the voltage profile of grid decreases which results in increase in voltage regulation and hence increase in line current. The increased line current helps to create a large amount of copper losses. So, to maintain and reduce copper losses, reactive power supply to grid is must. According to studies that shows reliance on large number of PEV connected, charger ratings in those PEVs, distribution transformer rating (25-100kVA), charging current harmonics and geographical location, the lifetime of distribution transformer can be reduced down to 26% of normal working life expectancy [5], [6]. The major advantage of large number of PEVs is that during peak load times the reactive power can be induced near to the load. The design of battery charger is of utmost importance to regulate the power flow, therefore,

Revised Manuscript Received on May 10, 2019.

Gaiffy Singla, Electrical & Instrumentation Engineering Department, Thapar Institute of Engineering and Technology, Patiala, India.

Surya Prakash, Electrical & Instrumentation Engineering Department, Thapar Institute of Engineering and Technology, Patiala, India

maintains reliable service of electric power. Since the origin of Electric Vehicles, there are many different charging strategies took place that is used to charge the PEV battery. With the time many different circuit charger topologies take place i.e. dedicated or integrated. Table Ishows the classification of charger on the basis of location (either on board or off board the vehicle), waveform type (either AC or DC), the direction of power flow (either unidirectional or bidirectional).

TABLE I
CHARGER CLASSIFICATION CHART

CLASSIFICATION	*SYMBOL*
TOPOLOGY	DEDICATED OR INTEGRATED
CONNECTION TYPE	CONDUCTIVE, MECHANICAL, INDUCTIVE
DIRECTION OF POWER FLOW	UNIDIRECTIONAL OR BIDIRECTIONAL
LOCATION	ON BOARD OR OFF BOARD
ELECTRICAL WAVEFORM	AC OR DC

Electric Vehicle batteries act as power storage devices to store the power in batteries for a particular interval of time and the stored power can be used when needed [7]. Charger plays an importunate role to the integration of EVs in the grid so as to demote the negative impact of congestion network of electric vehicles in charging station. The prime cons of EVs are its storage capability. Amid high load times the EVs feed stored power back to the grid and hence increases the efficiency of the distribution transformer (DT) and also alleviate the overloading of DT [6]. The costumers will be given a bonus for that [2], [8-10].

The two kinds of topologies are used for this purpose i.e. unidirectional charging and bidirectional charging. The unidirectional topology is Power Factor Corrected (PFC) topology used for unidirectional charging operation of the battery [11], [12]. The bidirectional topology uses single-phase ac-dc boost converter, which is also used for V2G purposes [13–15]. However, a unidirectional charger is used for only charging purpose i.e. Grid-to-Vehicle (G2V) mode. The change in P_{cmd} and Q_{cmd} will make changes in dc link voltage and further changes the charging current of battery. In this way, the battery charging is controlled. Reactive power assistance to the grid does not affect to the SOC of the battery but it does make changes in dc-link capacitors because more charging and discharging cycles are used [16].

In [17], [18], [19], and [20], mainly two controllers are utilized for ac-dc and dc-dc converters. The controller utilizes isolate references for AC–DC and DC–DC stages (i.e. P_{cmd}, Q_{cmd}, i_{bt*}). The controller in the system controls both converters, and consequently reclaims active power (P_{cmd}) and reactive power (Q_{cmd}) orders that must transmit between the EV and grid. The other signals can be obtained from the two reference signals (P_{cmd} and Q_{cmd}). The charger that is used to follow only P_{cmd} and Q_{cmd} is profitable for smart grid applications. The charger proposed in [2] requires large size of the DC-link capacitor, which results in limited reactive power output. The reactive power compensation depends upon the size of dc-link capacitor which further depends on the configuration used in the converter, size of the charger and the coupling inductor at the source side. The charger represented in [18] has slow very response for the commands given at, the source side. The SOC of the battery is skipped during reactive power compensation in this type of charger, which affects the performance of charger.

In this proposed work, the single phase PEV charger is developed and its block diagram has been presented. The charger consists of two converters and their corresponding controllers. In today's era electric vehicles are in trending position. However, the work done on low voltage supply to electric vehicles is very rare. Therefore, the authors are motivated to develop the pace in this work area so that low voltage applications can be applicable in rural and urban areas at rapid rate. The work on high voltage part has been done in large amount; therefore, there is a need to focus on low voltage side for charging the electric vehicles especially in domestic areas.

The proposed charger and its control strategy is developed in MATLAB SIMULINK. Section II portrays the converter working and its description. Section III is mainly focused on the design and working of controller. Section IV concentrates on simulation results of the proposed PEV charger.

II. DESCRIPTION OF PROPOSED PEV CHARGER CONVERTER

The charger proposed, has two stages which are AC-DC boost converter and the DC-DC buck converter as shown in Figure 1. The ac-dc full bridge boost converter is useful to transform low ac voltage (120V) into high dc

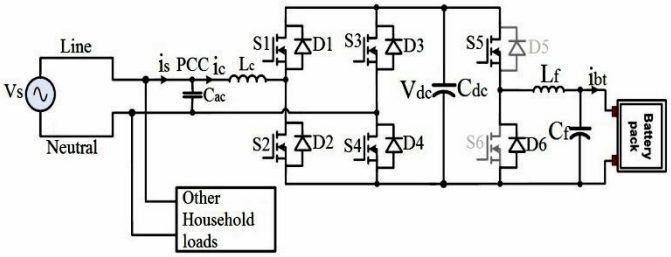

Figure 1: Battery Charger Circuit Diagram

voltage (400V) without using a transformer. The dc-dc buck converter is used to convert high dc link voltage into low battery voltage and dc-dc controller is also used to regulate the Battery Charging Current [16]. The prime motive of the charger is to charge the electric vehicle via proper coordination between EV and grid. The converters used in the charger consists of corresponding controllers. The ac-dc converter is experienced with bipolar modulation which means converter output is either $+V_{dc}$ or $-V_{dc}$. During the turn-on interval of switches S_1 and S_4, switches S_2 and S_3 remains switched off and vice-versa. MOSFET switches carry peak current equal to $\sqrt{2}I_c$ where I_c is RMS charging current. DC link voltage (V_{dc}) takes part in both ac-dc and dc-dc controllers and hence V_{dc} can be taken as a reference to control the battery charging current (i_{bt}). To obtain dc-dc buck operation switches S_5 and D_6 are switched on as shown in Figure 1. The charger operates in charging only mode. However, the inductor at grid side (L_{ac}) is habituated to boost up low ac grid voltage to high dc link voltage (V_{dc}) across dc link capacitor. During charging of battery, the presence of MOSFET switches causes large amount of switching losses. Due to this, the charger must have to follow P_{cmd} and Q_{cmd}, so that the input power must

be equal to output power without any loss.

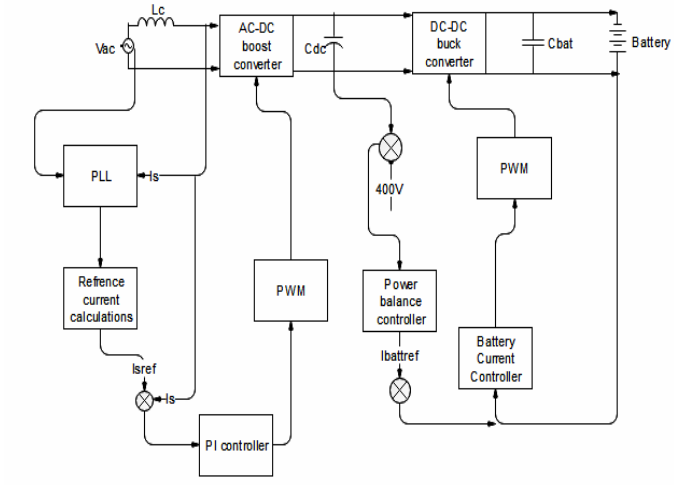

Figure 2: Complete Block Diagram of Proposed Charger

The values of inductor and capacitor components at battery side must be taken appropriately so as to reduce ripples in output waveforms. The lithium-ion battery is considered that operates in both CC and CV charging modes. Figure 2 represents the complete block diagram of a working charger. The charger used in is a unidirectional one and operates in G2V mode only. The charger follows P_{cmd} and Q_{cmd} for charging purpose. Any change in P_{cmd} and Q_{cmd} results in changing in DC link voltage and hence further changes the battery charging current. The modulation scheme used in ac-dc converter is bipolar modulation and in dc-dc converter is unidirectional modulation.

In general, two types of bidirectional chargers may be utilized; these include On-board and Off-board chargers. The on-board chargers can charge the batteries at any outlet which is available at either home or any workplace. The on-board chargers have limited power rating because of their limited size and dimensions; therefore, they take more time to charge the batteries [21]. The off-board chargers on the other hand are used for fast charging and take lesser time to charge a vehicle. The on board chargers have drawn more attention because of their low cost, easy availability, good efficiency and ease of use [22].

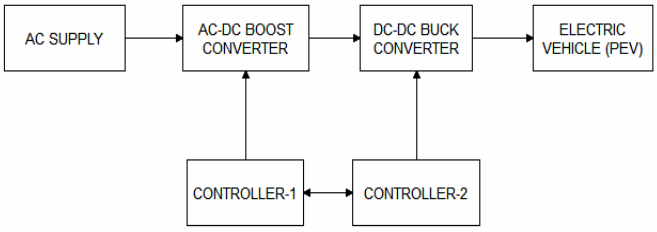

Figure 3: Schematic Block Diagram of Proposed Charger

Figure 3 shown above represents the schematic block diagram of proposed PEV charger. In this there are total six blocks and each block represents its own function. The supply carried from the grid is of alternating type i.e. ac supply. The supply carried away from grid utility is available at 120V or 230V. The ac supply passes through ac-dc converter and dc-dc converter and further to PEV battery. The PEV battery is a dc type battery which requires dc voltage and dc current. The ac-dc converter is regulated by ac-dc controller and dc-dc converter is regulated by dc-dc controller. After controlling the voltage and current, the power is transferred to electric vehicle battery (EV). The harmonics present in battery charging current must be less than 5%. To obtain this, source side inductance and capacitance values must be taken appropriately. The parameters used in 1.44kVA charger are shown in Table II. By using these parameters the required operation can be done.

TABLE II
PARAMETERS OF 1.44kVA CHARGER [16]

Parameters	***Symbol***	***Values***
Apparent power of the charger	S	1.44×10^3 VA
Supply Voltage	V_a	120 V RMS
Frequency	F	60 Hz
Supply-side inductance	L_c	1.0mH
Switching frequency for ac-dc converter	F_{sw1}	24×10^3 Hz
DC link voltage	V_{dc}	385 V
Switching frequency for dc-dc converter	F_{sw2}	42×10^3 Hz
DC link capacitance	C_{dc}	440×10^{-6} F
Filter capacitor (battery side)	C_f	190 µF
Filter inductance (battery side)	L_f	390 µH

III. DESIGN OF PROPOSED PEV CONTROLLER

In this research work, the PEV charger works only in first quadrant of P-Q plane. Therefore, the charger operates just in charging only mode. The G2V power flow is considered positive and V2G flow is considered as negative.

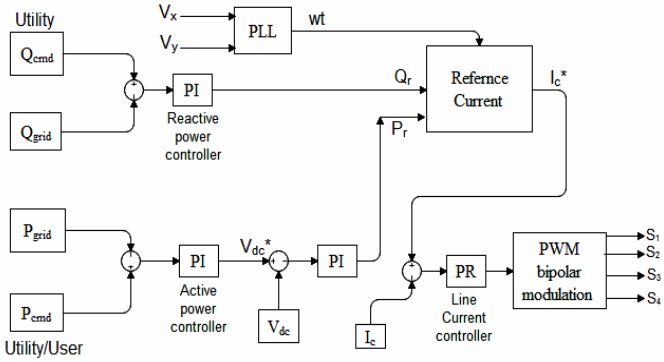

Figure 4: Block Diagram of Controller for AC-DC converter

Figure 4 represents the block diagram of ac-dc boost converter. In this the conversion of signals is done through p-q theory. This theory two voltage and current orthogonal signals are obtained by delay function. After that the output of instantaneous p-q block passes through low pass filters. The function of low pass filters is to demote the ripples inherit in it. After that the output P and Q are equated with P_{cmd} and Q_{cmd} provided by user/utility. The delayed (Orthogonal) signals are used for PLL algorithm(Phase locked loop) algorithm that tracks the phase angle of line voltage and induce the reference phase signal for battery charging current. The sensed signals are holded up for atleast one quarter to generate orthogonal signals. The ac-dc boost converter controls the dc link voltage (V_{dc}). The active power command (P_{cmd}) is used as reference power for purpose of battery charging. The difference between output powers and command powers further passes through two different PI controllers i.e. active and reactive power controllers. The main function of PI controllers is to demote the steady state error.Further there are two loops which

acts as feedback loop i.e. P-loop and Q-loop. The output of P-loop (V_{dc}*) is compared with dc link voltage (V_{dc}). The difference between actual and reference signals further passes through dc voltage controller (PI Controller) which produce power called P_r. Q_r in Q loop is produced as same as in case of P-loop. The main function of these two signals is to produce reference charging current (i_c*). The reference charging current is further compared with actual charging current (i_c). The difference between these two parameters results in an error and this is further sent to PR controller to control the charging current [23]. After this the charging current passes through bipolar modulation. The yield of bipolar modulation results in gate pulses for switches. Hence in this way AC–DC converter controller controls the charging current by applying gate pulses to the switches.

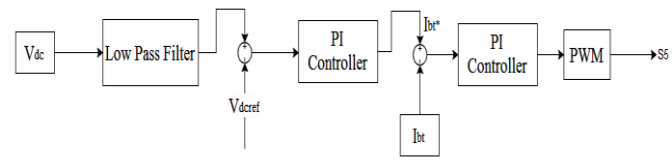

Figure 5: Block Diagram of Controller for DC-DC converter

Figure 5 represents the block diagram of dc-dc converter.The DC-DC buck converter is used to reduce the dc link voltage to battery voltage so that charging current must flow from high voltage to low voltage i.e. from dc link capacitor to PEV battery. The DC-DC converter must have a controller that controls the above process. In this controller the sensed dc link voltage must proceed through low pass filter that helps to reduce ripples in it. The reference dc link voltage (V_{dc}*) is equated with sensed dc link voltage (V_{dc}).The difference between actual and reference signals passes through power balance controller (PI controller). The PI controller outputs a reference charging battery current (i_{bt}*). The sensed battery charging current is equated with reference charging current of battery (i_c*) [24]. The obtained result is regulated with battery current controller (PI Controller). Pulse Width Modulation (PWM) block recieves the output signal of battery current controller (PI Controller) and generates duty cycle (S_5) consequently.

IV CONTROL METHODOLOGY

A. PI (Proportional Integral) Controller

The Proportional and integral (PI) refers to integration of error signal for a period of time. Error signal is proportional to rate of change of correcting signal. Figure 6 represents the block diagram of PI controller.

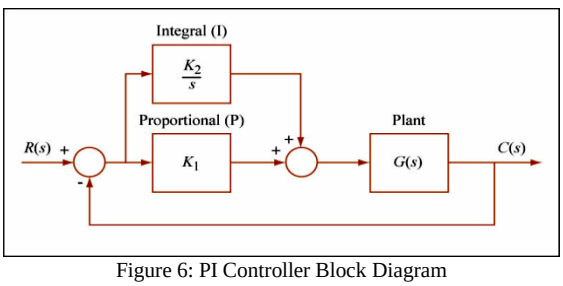

Figure 6: PI Controller Block Diagram

Transfer function of the PI controller is given as follows:

$$G(s) = K_p + \frac{K_i}{s} \qquad (1)$$

Where K_p is the constant of proportionality and K_i is the integral gain of the PI controller. The controller will perform until error is completely removed. The difference between generation and demand will produce error. The steady state error is reduced with the help of PI controller and at the same time reduces the settling time.

The p-q theory is used to calculate P and Q. The 'x' components are indicators of sensed signals. The 'y' signals are produced by delay function. The orthogonal signals (y) are delayed by one-quarter of grid period which is equal to (1/240) corresponds to 100 samples with 24 kHz sampling frequency [25]. The signals are delayed for utilization in PLL algorithm which tracks phase angle of line voltage and produces a reference signal for charging current. The single-phase active is given by:

$$P = \frac{1}{2}\left(V_x \times I_x + V_y \times I_y\right) \qquad (2)$$

$$Q = -\frac{1}{2}\left(V_x \times I_y + V_y \times I_x\right) \qquad (3)$$

There are two low pass filters that are used to yield P and Q outputs. The active power command (P_{cmd}) is given by the client and reactive power command (Q_{cmd}) is provided by utility/grid. The charger must have to follow these power commands for efficient operation. During peak load hours grid can regulate P_{cmd} to harmonize charging power [22]. If any client or costumer provides reactive power to the grid then grid must provide an incentive to the costumer. However, P_{cmd} and Q_{cmd} must be examined before being sent to the charger.

The active power (P) must be matched with active power command (P_{cmd}) to fulfil the desired operation. This can be by changing dc link voltage (V_{dc}*). The loop equation for this is as follows:

$$V_{dc}^* = \left(K_p^a + \frac{K_i^a}{s}\right) \times (P_{cmd} - P) \qquad (4)$$

The dc voltage loop (v-loop) follows dc link voltage (V_{dc}*). The difference of sensed dc link voltage and reference dc link voltage passes through PI controller. The constants of the controller are changed accordingly to match the actual and reference value. This loop's output produces reference tracking active power (P_r). The equation for this is as follows:

$$P_r = (K_p^b + \frac{K_i^b}{s}) \times (V_{dc}^* - V_{dc}) \qquad (5)$$

The output Q is matched with Q_{cmd} from the grid with the help of reactive power loop (Q-loop). The mismatch between actual reactive power (Q) and reactive power command (Q_{cmd}) is passed through PI controller whose constants have to be modified to match the sensed and reference reactive power (Q_r). The equation for Q-loop is as follows:

$$Q_r = \left(K_p^c + \frac{K_i^c}{s}\right) \times (Q_{cmd} - Q) \qquad (6)$$

Q-loop tells whether the charger can supply or sink the reactive power. The reference charging current is induced by yields of dc voltage loop and reactive power loop. The following equations are also used to calculate reference charging current (i_c*).

$$\emptyset = \tan^{-1}\frac{Q_r}{P_r} \qquad (7)$$

$$I_c = \frac{P_r}{V_a \cos \emptyset} \qquad (8)$$

And finally

$$i_c^* = \sqrt{2} I_c \sin(\omega t - \emptyset) \quad (9)$$

Where I_c is the RMS value of charging current. V_a is the source voltage.

B. PR (Proportional Resonant) controller

The transfer function of PR controller is:

$$G_{PR} = K_P + \frac{2K_r s}{s^2 + \omega_1^2} \quad (10)$$

where *Kp* is the proportional gain and ω_1, *Kr* are the resonant frequency and gain, respectively. The PR controller provides an infinite gain at resonant frequency and zero phase shift. However, PR controller is used to regulate the mismatch between reference charging current (i_c*) and sensed charging current (i_c) [26]. The difference between two charging currents are fed to PR controller whose constants are changed to match the sensed and reference charging current. The PR controller used in this charging system provides smoothness in charging of battery as compared to controllers used by other authors. This is the novelty of this work. The PR controller is infinite gain controller especially used for controlling the charging current. Hence this controller brings the novelty in this charging system. The PR controller yield is used to produce duty cycle (*d*) for an ac-dc converter [27]. The equation for i-loop is as follows:

$$d = (K_p^d + \frac{2K_i^d \omega_c s}{s^2 + 2\omega_c s + \omega^2}) \times (i_c^* - i_c) \quad (11)$$

For dc-dc converter, the reference dc link voltage (V_{dc}*) is equated with V_{dc}. The resultant error passes through power balance controller (PI) controller. The constants of PI controller are modified to remove the mismatch between sensed and reference dc link voltage. The output of PI controller yields reference battery current (i_{bt}*). The equation for this is as follows:

$$i_{bt}^* = \left(K_p^e + \frac{K_i^e}{s}\right) \times \left(V_{dc} - V_{dcref}\right) \quad (12)$$

The loop represented above is used to maintain the input-output balance of power. The main purpose of this loop is to fulfil P_{cmd} so as to charge the battery without any loss. The equation for this loop is as follows:

$$d_o = \left(K_p^f + K_i^f\right) \times \left(i_{bt}^* - i_{bt}\right) \quad (13)$$

where d_0 is the duty cycle.

In this framework, battery charging current is induced by varying the output voltage of ac –dc boost converter. If there is increase in value of P_{cmd} then V_{dc} also increases to a new benchmark and vice-versa. This small change in V_{dc} yields a change in i_{bt}. Second order harmonics present in DC link voltage are filtered using low pass filters whose transfer function is given below.

$$H(s) = \frac{k\omega_{c1}^2}{s^2 + 2\varepsilon\omega_{c1} s + \omega_{c1}^2} \quad (14)$$

where $\omega_{c1}=2\pi f_c$, $f_c=20$Hz and $\varepsilon=\sqrt{2}$.

Table III represents the values of parameters of controller used in above equations. By using these parameters the battery charging current can be controlled.

TABLE III
LIST OF CONTROLLER PARAMETERS [16]

Parameters	*Symbol*	*Value*
Angular frequency	ω	377 rad/s
Crossover angular frequency	ω_c	3.1 rad/s
Proportional const. for current loop (I loop) controller (P-R)	K_p^d	1.2
Integral constant for current loop (i-loop) controller (P-R)	K_i^d	1000
Proportional const. for dc voltage loop (v-loop) controller (PI)	K_p^b	1.5
Integral constant for dc voltage loop (v-loop) controller (PI)	K_i^b	100
Proportional const. for reactive power loop (Q-loop) controller (PI)	K_p^c	0.2
Integral constant for reactive power loop (Q-loop) controller (PI)	K_i^c	30
Proportional const. for active power loop (P-loop) controller (PI)	K_p^a	1
Integral const. for active power loop (P-loop) PI contr.	K_i^a	20
Proportional constant for balance loop controller (PI)	K_p^e	0.045
Integral constant for balance loop controller (PI)	K_i^e	0.5
Proportional constant for battery current (i_{bt}) loop controller (PI)	K_p^f	0.15
Integral constant for battery current (i_{bt}) loop controller (PI)	K_i^f	10

The parameters for 6.6kVA charger is shown in Table IV. These values are most suitable for making 6.6kVA charger.

TABLE IV
PARAMETERS OF 6.6KVA CHARGER [26]

Parameters	*Symbol*	*Values*
Apparent power of the charger	S	6.6×10^3 VA
Supply Voltage	V_a	230 V RMS
Frequency	F	60 Hz
Supply-side inductance	L_c	1.5mH
Switching frequency for ac-dc converter	F_{sw1}	24×10^3 Hz
DC link voltage	V_{dc}	390 V
Switching frequency for dc-dc converter	F_{sw2}	42×10^3 Hz
DC link capacitance	C_{dc}	860×10^{-6} F
Filter capacitor (battery side)	C_f	200 µF
Filter inductance (battery side)	L_f	690 µH

V. SIMULATION RESULTS OF PROPOSED ELECTRIC VEHICLE CHARGER

The results obtained from the simulation of single phase PEV charger are represented in Fig. 7-18. There are three types of chargers used for the charging of electric vehicle battery.

A. 5.1 1.44kVA Charger

As explained above the charger works in charging only mode i.e. active power command is positive and reactive power command is zero. The G2V power flow is considered positive. Normally the battery voltage taken is between 320V-390V. Initially the battery SOC is 20%. The nominal battery voltage is 365V and battery current is

3.8A which makes the charging power equals to 365V * 3.8A = 1440VA. Figure 7 represents the source voltage for 1.44kVA charger. The RMS source voltage is 120V and its peak value is 170V.The simulation of the charger is done for 3 seconds. The RMS charging current is 12A. The charger is required to follow the commands given by grid or user.

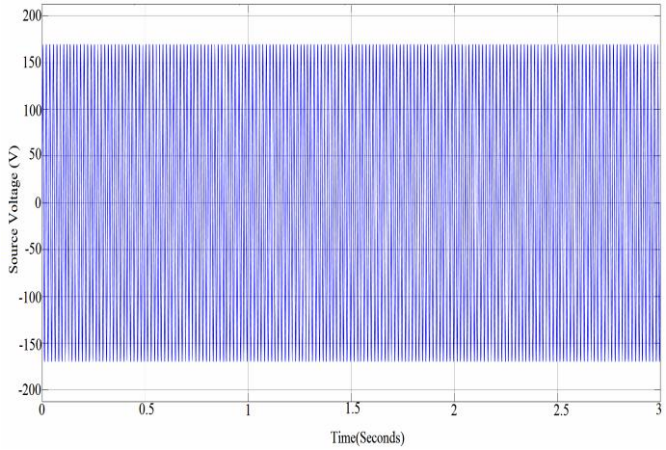

Figure 7: Source Voltage for 1.44kVA charger

Figure 8 represents the battery charging current. Its value is 3.8A.

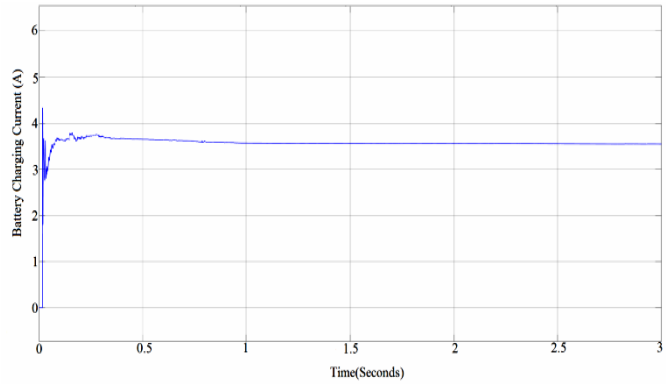

Figure 8: Battery Charging Current for 1.44kVA charger

Figure 9 shows the dc link voltage for 1.44kVA charger. The ac input supply is boosted up with the help of boost converter to maintain the dc link voltage near about 390V. The battery nominal voltage is 365V. The ac supply is boosted up so that the current can be conveyed from dc link capacitor to the EV battery for charging purpose.

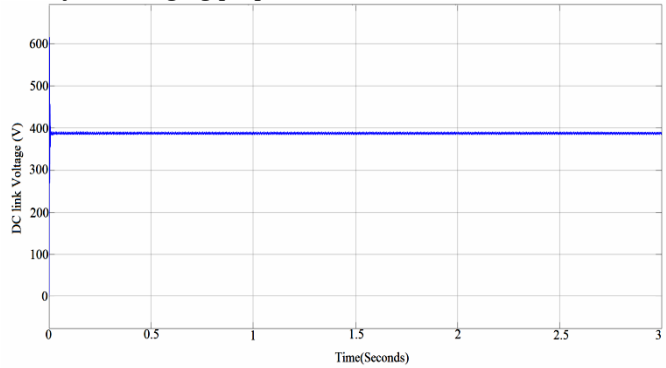

Figure 9: DC link Voltage for 1.44kVA charger

Figure 10 shows the SOC of the battery. Out of three chargers the 6.6kVA charger is swiftest. The 6.6kVA charger takes approximately one-fourth time against 1.44kVA charger to charge the battery.

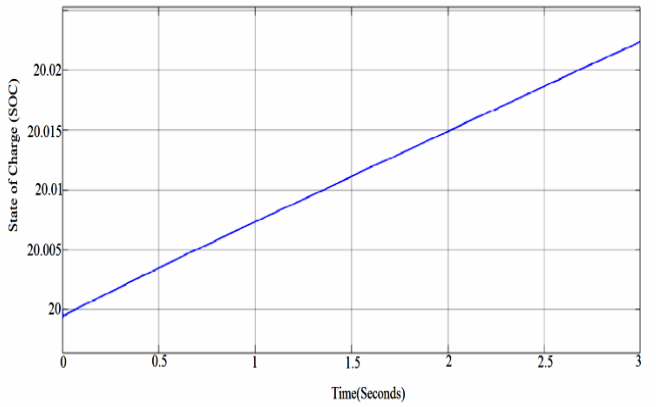

Figure 10: State of Charge (SOC) for 1.44kVA charger

B. 5.2 3.3kVA Charger

In this type of charger, the source voltage taken is 230V RMS. The RMS value of line current is 17A.The outputs of source voltage, V_{dc}, i_{bt}, and SOC of battery are shown below. Figure 11 shows AC source voltage for 3.3kVA charger. The RMS value of source voltage is 230V and its peak value is 310V.

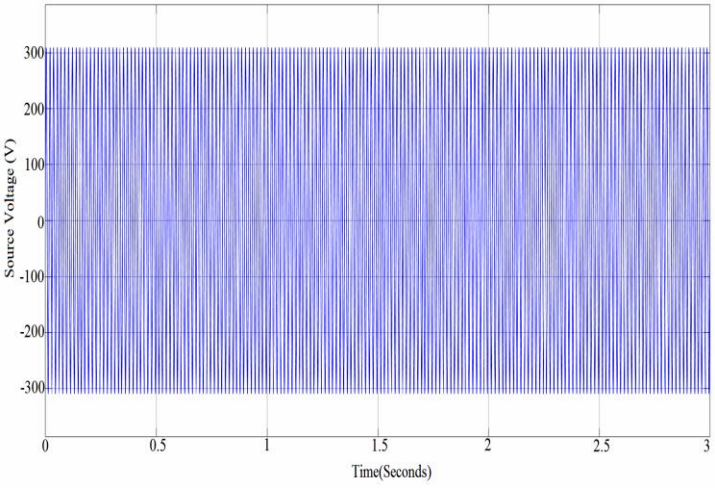

Figure 11: Source Voltage for 3.3kVA charger

Figure 12 represents dc link voltage for 3.3kVA charger. The value of dc link voltage is 390V.

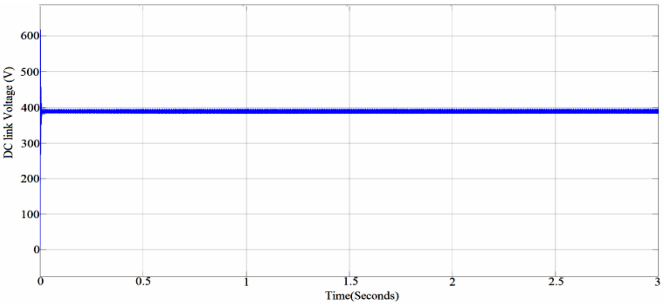

Figure 12: DC link Voltage for 3.3kVA charger

Figure 13 represents the battery charging current for 3.3kVA charger. The RMS value of battery charging current is 9A. The battery capacity used here is 12Ah.

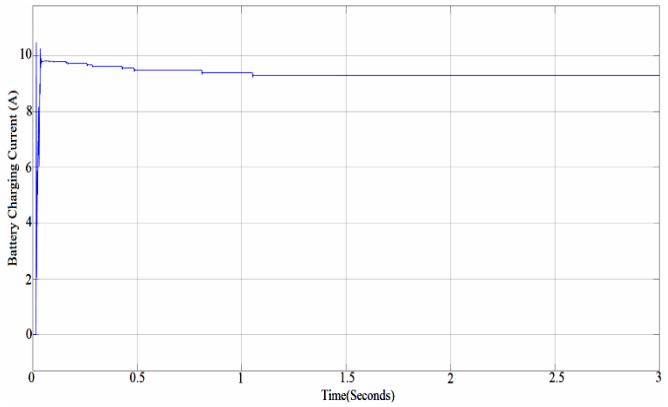

Figure 13: Battery Charging Current for 3.3kVA charger

Figure 14 represents the SOC of the battery. The 3.3kVA charger is fast as compared to 1.44kVA charger. The comparison between their SOCs is shown in Figures 9, 13, and 17.

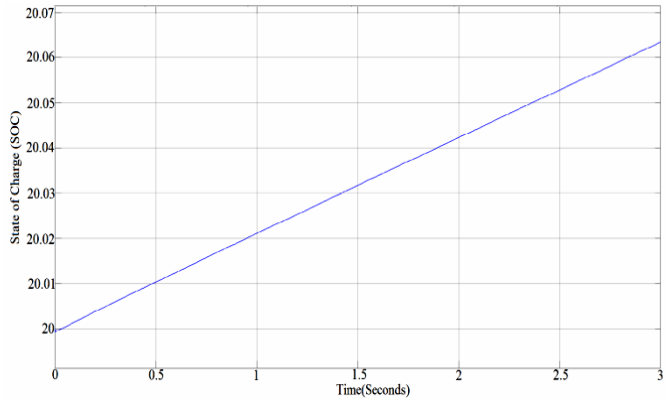

Figure 14: State of Charge (SOC) for 3.3kVA charger

C. 5.3 6.6kVA Charger

This kind of charger also falls in the category of Level-2 charging system. It is a low voltage charging system which is beneficial for charging the battery in domestic and rural areas. Figure 15 represents the source voltage for 6.6kVA charger. The RMS value of source voltage is 230V and its peak value is 310V.

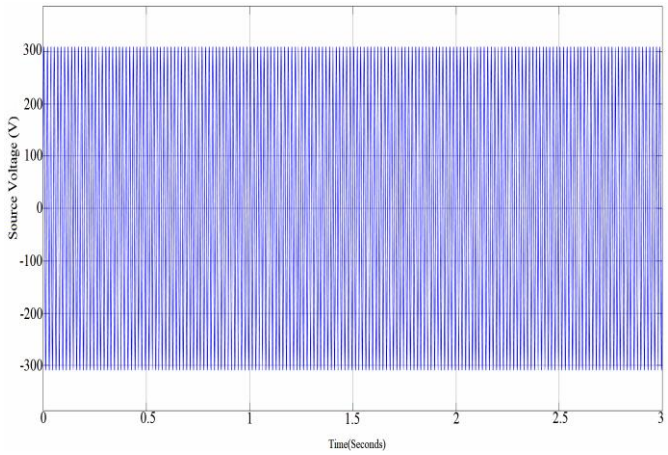

Figure 15: Source Voltage for 6.6kVA charger

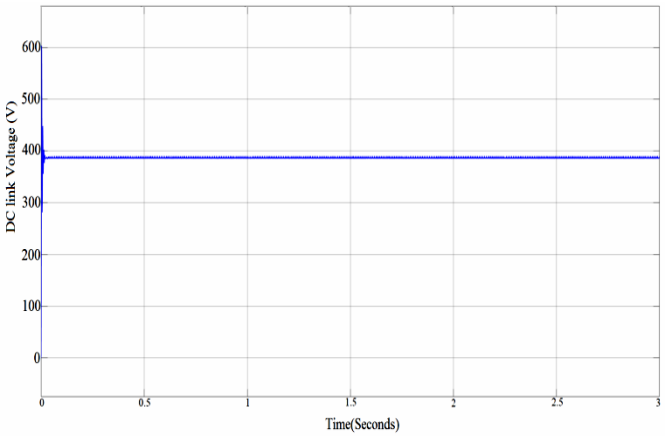

Figure 16: DC link Voltage for 6.6kVA charger

Figure 16 and Figure 17 represent the dc link voltage and battery charging current respectively. The RMS value of Battery charging current is 18A. The nominal battery voltage is 365V.

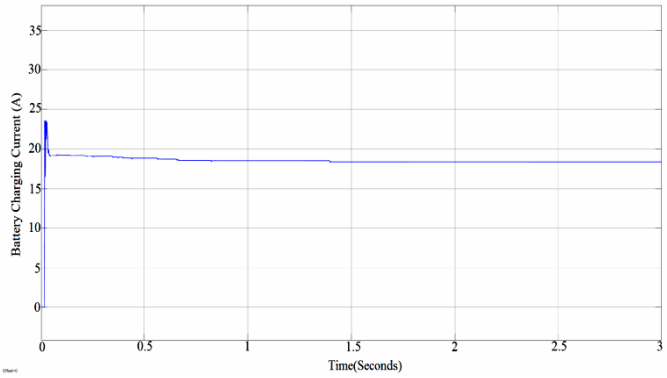

Figure 17: Battery Charging Current for 6.6kVA charger

Figure 18 represents the state of charge of the battery for 6.6kVA charger.

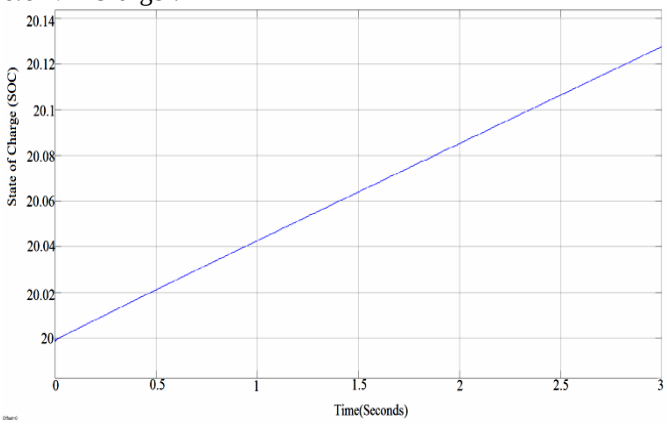

Figure 18: State of Charge (SOC) for 6.6kVA charger

The SOC waveform shows that the 6.6kVA charger is fast as compared to 1.44kVA and 3.3kVA charger. Table V portrays the comparison between three types of chargers.

TABLE V
COMPARISON OF THREE TYPES OF CHARGER

	Level-1 1.44kVA Charger	Level-2 3.3kVA Charger	Level-2 6.6kVA Charger
Supply Voltage	120V RMS	230V RMS	230V RMS
Line Current	12A RMS	17A RMS	24A RMS
DC link Voltage	385V	390V	390V
Battery charging current	3.8A	9A	18A

VI. CONCLUSION

This work mainly concentrates on the charging of the electric vehicles through single phase PEV transformer less charger. The two controllers used in this charger is used to regulate the battery charging current. The change in P_{cmd} and Q_{cmd} yields the changes in battery charging current (i_{bt}). There are three types of chargers used i.e. i) Level-1 1.44kVA charger ii) Level-2 3.3kVA charger iii) Level-2 6.6kVA charger. The outputs of these chargers are shown in Fig.7 to Fig.18 in section IV. The Table III shown above represents the values used in controller for controlling the charging of the electric vehicle battery. The simulation result shows the comparison of three types of chargers in terms of fast and efficient charging. Table V also represents the comparison between various types of controllers. The simulation results show that 6.6kVA charger is much faster than 1.44kVA charger and 3.3kVA charger which is better result compared to [16].

REFERENCES

1. M. C. Kisacikoglu, A. Bedir, B. Ozpineci, and L. M. Tolbert, "PHEV-EV charger technology assessment with an emphasis on V2G operation," Oak Ridge Nat. Lab., Oak Ridge, TN, USA, Tech. Rep. ORNL/TM-2010/221, Mar.2012.
2. Z. Luo, Z. Hu, Y. Song, Z. Xu, and H. Lu, "Optimal coordination of plug-in electric vehicles in power grids with cost-benefit analysis part I: Enabling techniques," IEEE Trans. Power Systems, vol. 28, no. 4, pp. 3546–3555, Nov. 2013.
3. D. Manzet al., "The grid of the future: Ten trends that will shape the grid over the next decade," IEEE Power Energy Mag., vol. 12, no. 3, pp. 26–36, May 2014.
4. M. C. Kisacikoglu, B. Ozpineci, and L. M. Tolbert, "EV/PHEV bidirectional charger assessment for V2G reactive power operation," IEEE Trans. Power Electron., vol. 28, no. 12, pp. 5717–5727, Dec. 2013.
5. M. Kuss, T. Markel, and W. Kramer, "Application of distribution transformer thermal life models to electrified vehicle charging loads using monte-carlo method," in Elect. Vehicle Symp, Shenzen, China, Nov. 5–9 2010.
6. R. Moghe, F. Kreikebaum, J. E. Hernandez, R. P. Kandula, and D. Divan, "Mitigating distribution transformer lifetime degradation caused by grid-enabled vehicle (GEV) charging," IEEE Energy Conversion Congr. Expo. (ECCE), Phoenix, AZ, 2011, pp. 835–842.
7. T. S. Bryden, A. J. Cruden, G. Hilton, B. H. Dimitrov, C. P. de Le´on, and A. Mortimer, "Off-vehicle energy store selection for high rate ev charging station," 6th Hybrid and Electric Vehicles Conference (HEVC 2016), pp. 1–9, Nov 2016.
8. K. Mets, T. Verschueren, F. D. Turck, and C. Develder, "Exploiting V2Gto optimize residential energy consumption with electrical vehicle (dis)charging," IEEE First International Workshop on Smart Grid Modeling and Simulation (SGMS), pp. 7–12 Oct 2011.
9. H. Liu, Z. Hu, Y. Song, and J. Lin, "Decentralized vehicle-to-grid control for primary frequency regulation considering charging demands," IEEE Transactions on Power Systems, vol. 28, no. 3, pp. 3480–3489, Aug 2013.
10. S. Vandael, T. Holvoet, G. Deconinck, S. Kamboj, and W. Kempton, "A comparison of two given mechanisms for providing ancillary services at the university of delaware," IEEE International Conference on Smart Grid Communications (Smart Grid - Comm), pp. 211–216, Oct 2013.
11. F. Musavi, M. Edington, W. Eberle, and W. G. Dunford, "Energy efficiency in plugin hybrid electric vehicle chargers: Evaluation and comparison of front end ac-dc topologies," IEEE Energy Conversion Congress and Exposition, pp. 273–280, Sept 2011.
12. A. Khaligh and S. Dusmez, "Comprehensive topological analysis of conductive and inductive charging solutions for plug-in electric vehicles," IEEE Transactions on Vehicular Technology, vol. 61, no. 8, pp. 3475–3489, Oct 2012.
13. M. Yilmaz and P. T. Krein, "Review of battery charger topologies, charging power levels, and infrastructure for plug-in electric and hybrid vehicles," IEEE Transactions on Power Electronics, vol. 28, no. 5, pp. 2151–2169, May 2013.
14. B. Singh, B. N. Singh, A. Chandra, K. Al-Haddad, A. Pandey, and D. P. Kothari, "A review of single-phase improved power quality ac-dc converters," IEEE Transactions on Industrial Electronics, vol. 50, no. 5, pp. 962–981, Oct 2003.
15. D. C. Erb, O. C. Onar, and A. Khaligh, "Bi-directional charging topologies for plug-in hybrid electric vehicles," Twenty-Fifth Annual IEEE Applied Power Electronics Conference and Exposition (APEC), pp. 2066–2072, Feb 2010.
16. Kisacikoglu, Mithat C., Metin Kesler, and Leon M. Tolbert. "Single phase on-board bidirectional PEV charger for V2G reactive power operation." IEEE Transactions on Smart Grid, vol. 6, no. 2, pp. 767-775, 2015.
17. J. G. Pinto, V. Monteiro, H. Goncalves, and J. L. Afonso, "On-board reconfigurable battery charger for electric vehicles with traction-to-auxiliary model," IEEE Trans. Vehicle Technology, vol. 63, no. 3, pp. 1104–1116, Mar. 2014.
18. T. Tanaka, T. Sekiya, H. Tanaka, M. Okamoto, and E. Hiraki, "Smart charger for electric vehicles with power-quality compensator on single phase three-wire distribution feeders," IEEE Trans. Ind. Appl., vol. 49, no. 6, pp. 2628–2635, Nov./Dec. 2013.
19. K.-W. Hu and C.-M. Liaw, "On a bidirectional adapter with G2B charging and B2X emergency discharging functions," IEEE Trans. Ind. Electron., vol. 61, no. 1, pp. 243–257, Jan. 2014.
20. A. Arancibia, K. Strunz, and F. Mancilla-David, "A unified single and three-phase control for grid connected electric vehicles," IEEE Trans. Smart Grid, vol. 4, no. 4, pp. 1–11, Dec. 2013.
21. "Nissan Leaf Electric Car," 2016. [Online]. Available: https://www.nissanusa.com/ electric-cars/leaf.
22. M. C. Kisacikoglu, B. Ozpineci, and L. M. Tolbert, "Examination of a PHEV bidirectional charger for V2G reactive power compensation," in Proc. IEEE Appl. Power Electron. Conf. Expo. (APEC), Palm Springs, CA, USA, pp. 458–465, Feb. 2010.
23. R. Teodorescu, F. Blaabjerg, M. Liserre, and P. C. Loh, "Proportional-resonant controllers and filters for grid-connected voltage-source converters," IEE Proceedings - Electric Power Applications, vol. 153, no. 5, pp. 750–762, September 2006.
24. A. Timbus, M. Liserre, R. Teodorescu, P. Rodriguez, and F. Blaabjerg, "Evaluation of current controllers for distributed power generation systems," IEEE Transactions on Power Electronics, vol. 24, no. 3, pp. 654–664, March 2009.
25. H. Akagi, Y. Kanazawa, and A. Nabae, "Instantaneous reactive power compensators comprising switching devices without energy storage components," IEEE Transactions on Industry Applications, vol. IA-20, no. 3, pp. 625–630, May 1984.
26. Kisacikoglu, Mithat Can. "Vehicle-to-grid (V2G) reactive power operation analysis of the EV/PHEV bidirectional battery charger." 2013.
27. R. Teodorescu, F. Blaabjerg, M. Liserre, and P. Loh, "Proportional-resonant controllers and filters for grid-connected voltage-source converters," IEE Proc. Electric Power Applications, vol. 153, no. 5, pp. 750–762, Sep. 2006

AUTHORS PROFILE

Gaiffy Singla received his B. Tech. degree in Electrical Engineering from Punjab technical University, Punjab and M Tech. in power system from Thapar Institute of Engineering and Technology, Patiala- Punjab.

Surya Prakash received his Bachelor of Engineering degree from The I E (India) in 2003, He obtained his M. Tech. in Electrical Engg.(Power System) from KNIT, Sultanpur-India in 2009 and Ph. D in Electrical Engg.(Power System) from, SHIATS-DU(Formerly AAI-DU, Allahabad- India) in 2014. Presently he is working as Asst. prof. in the department of Electrical & Instrumentation Engineering, Thapar Institute of Engineering & Technology, Patiala. His field of interest includes power system operation & control, Artificial Intelligent control, distributed generation.